Effects of μCT radiation on tissue engineered bone-like constructs

Thomas P. Kraehenbuehl[1,a], Martin Stauber[1], Martin Ehrbar[2], Franz Weber[2], Heike Hall[3] and Ralph Müller[1,*]

[1] Institute for Biomechanics, ETH Zurich, Zurich, Switzerland

[2] Section Bioengineering and Department of Craniomaxillofacial Surgery, University Hospital, Zurich, Switzerland

[3] Department of Materials, ETH Zurich, Zurich, Switzerland

Abstract

High-resolution, non-destructive imaging with micro-computed tomography (μCT) enables *in situ* monitoring of tissue engineered bone constructs. However, it remains controversial, if the locally imposed X-ray dose affects bone development and thus could influence the results. Here, we developed a model system for μCT monitoring of tissue engineered bone-like constructs. We examined the *in vitro* effects of high-resolution μCT imaging on the cellular level by using pre-osteoblastic MC3T3-E1 cells embedded into three-dimensional collagen type I matrices. We found no significantly reduced cell survival 2 h after irradiation with a dose of 1.9 Gy. However, 24 h post-irradiation, cell survival was significantly decreased by 15% compared to non-irradiated samples. The highest dose of 7.6 Gy decreased survival of the pre-osteoblastic MC3T3-E1 cells by around 40% at 2 days post-irradiation. No significant increase of alkaline phosphatase (ALP) activity at 2 days post-irradiation was found with a dose of 1.9 Gy. However, ALP activity was significantly decreased after 7 days. Using our model system, the results indicate that μCT imaging with doses as low as 1.9 Gy, which is required to obtain a reasonable image quality, can induce irreparable damages on the cellular level.

Keywords: alkaline phosphatase activity (ALP); cell survival; collagen; MC3T3-E1 pre-osteoblastic cells; micro-computed tomography (μCT); tissue engineering.

[a] Present address: Hoffmann-La Roche, Translational Research Sciences, Nutley, NJ 07110, USA.

*Corresponding author: Ralph Müller, PhD, Institute for Biomechanics, Wolfgang-Pauli-Strasse 10, 8093 Zurich, Switzerland
Phone: +41-44-63245 92
Fax: + 41-44-63212 14
E-mail: ram@ethz.ch

Introduction

In vitro engineering of functional tissue constructs has gained importance in the past decade as the shortage of organs and tissues for transplantation increased [21], but also for safety and efficacy testing of new therapeutics [8, 12, 15]. So far, quality testing of engineered tissue constructs relied on destructive techniques including reverse transcription polymerase chain reaction to analyze gene expression or histology to assess organization and integrity of the tissue. Thus, monitoring over time and functional optimization in response to assessed changes in tissue morphology and functionality was not possible with these techniques. Other methods, such as magnetic resonance imaging or positron emission tomography, do not provide sufficient spatial resolution [10, 17].

Micro-computed tomography (μCT) was shown to be useful as a non-destructive method in imaging three-dimensional (3D) bone microarchitecture at resolutions in the order of 10 μm in relatively short acquisition time (5–30 min) and at low cost [2, 3, 19]. In recent studies, μCT was used to monitor the development of 3D *in vitro* engineered bone-like tissues [4, 13, 14], cartilage-like tissues [23] or skin-like layers [20] over time. However, one drawback of obtaining high-quality μCT images can be the locally deposed radiation dose and its potential effect on cell survival, cell functionality and cell development [11].

Several studies have examined the effects of ionizing radiation on bone cells in a two-dimensional (2D) environment at doses up to 8 Gy [5, 6, 9]. Although the proliferation of MC3T3-E1 pre-osteoblastic cells and osteoblast-like cells from the rat calvarium was not affected by a radiation dose of 0.4 Gy, a dose of 4.0 Gy significantly decreased proliferation in all studies, and in some cases significantly altered alkaline phosphatase (ALP) activity, collagen production and vascular endothelial growth factor secretion as compared to non-irradiated control samples. However, irradiation effects on 3D tissue engineered constructs, which mimic native 3D tissue and organ structures better than 2D environments [8, 12], are not fully understood. Specifically, the critical dose, which can maximally be deposited onto the constructs without inducing cellular damages, is not clear. Because there is a big difference between a flat layer of cells and a complex 3D tissue [1], it is important to investigate the irradiation effect in 3D tissues.

The aim of this study was to assess this maximum dose. We have developed a model system for μCT monitoring of 3D tissue engineered constructs and to elucidate effects of the ionizing radiation applied by μCT imaging on the cellular level by using MC3T3-E1 pre-osteoblastic cells embedded in 3D collagen type I matrices mimicking bone-like tissue [7, 16]. We hypothesized that the locally deposed X-

ray dose by high-resolution µCT imaging can cause alterations on the cellular level in a dose- and time-dependent manner. This not only can affect the development of engineered 3D tissue constructs for clinical applications but also the results of pharmaceutical studies for testing new therapeutics.

Materials and methods

Dose measurement with thermoluminescent detectors

The radiation dose occurring with typical settings for µCT scanning was measured with thermoluminescent detectors (TLDs) made of lithium fluoride powder embedded in a glass tube of 12 mm length and 1.4 mm diameter (TLD-700, Harshaw/Filtrol, Solon, OH, USA). For µCT measurement, the TLDs were placed in a cylindrical polymethyl methacrylate (PMMA) cylinder (inner diameter: 2 mm, outer diameter: 8 mm) to ensure corresponding radiation doses as applied to the cells embedded into the collagen matrix. The µCT (µCT40, Scanco Medical AG, Brüttisellen, Switzerland) was operated at a peak voltage of 50 kV with an integration time of 100 ms in all possible scanning modes. The three primary scanning modes provided by the µCT manufacturer were ''standard resolution'' mode (250 projections/180°, 1024 samples per projection), ''medium resolution'' mode (500 projections/180°, 1024 samples), and ''high resolution'' mode (1000 projections/180°, 2048 samples). In each mode, five different nominal resolutions were available namely 12, 16, 20, 30, and 36 µm for the standard and medium resolution mode, and 6, 8, 10, 15, and 18 µm for the high resolution mode. These nominal resolution values correspond to the settings that can be chosen to run the scans and do not represent the actual spatial resolution, which is typically lower. The best spatial resolution (10% MTF) at 6 µm voxel size is specified by the manufacturer to be 10 µm. After irradiation, the TLDs were read out with a photo-multiplier using a standard heating protocol.

For all cell experiments the medium resolution mode at 20 µm nominal resolution was used, but with a threefold increased integration time resulting in a calculated base dose of 1.9 Gy per measurement. To achieve the higher doses of 3.8, 5.7, and 7.6 Gy, the base measurement was repeated 2, 3, and 4 times, respectively. The total times for application of these radiation doses were 1.5 h, 3 h, 4.5 h, and 6 h, respectively. To examine potential differences in image quality, a bovine trabecular bone sample was scanned with µCT in four different modes: in standard resolution mode at 30 µm and 16 µm nominal resolution, as well as in high resolution mode at 15 µm and 8 µm nominal resolution.

Culture of pre-osteoblastic MC3T3-E1 cells

A MC3T3-E1 subclone 24 (LGC Promochem Sarl, Molsheim Cedex, France) was cultured between passage 6–10 in alpha-modified minimum essential medium containing 10% fetal bovine serum (both Invitrogen, Basel, Switzerland),

1 µg/ml bone morphogenic protein-2 produced as previously shown [22], and 25 mmol 4-(2-hydroxyethyl)-1-piperazine-ethanesulfonic acid (Sigma-Aldrich, Buchs, Switzerland).

Preparation of 3D collagen matrices

Collagen type I matrices (Vitrogen 100, Cohesion, Palo Alto, CA, USA) of 2 mg/ml were used. Matrix formation was initiated by raising the pH to physiological conditions (pH 7.4) by adding 0.1 M NaOH to the collagen solution. To ensure homogeneous cell encapsulation, the matrices were presolidified at 37°C for 5 min prior to the addition of 500,000 cells/ml collagen I. Matrices with a volume of 30 µl were then filled into sterilized (70% ethanol, exposure to UV light) PMMA sample holders with a capacity of 35 µl and incubated for 30 min at 37°C to solidify. The sample holders containing the 3D cell cultures were then kept in 1 ml medium in a well of a 24-well plate under standard cell culture conditions.

Irradiation with µCT

A high-resolution micro-computed tomography system (µCT40, Scanco Medical AG, Brüttisellen, Switzerland) was used to apply the ionizing radiation to the cells embedded in the 3D collagen type I matrices. The system was operated in all cell experiments at a peak voltage of 50 kV with an integration time of 300 ms at a nominal resolution of 20 µm. The absolute dose delivered to the samples was assessed in an independent experiment using TLDs. In all experiments, cultured MC3T3-E1 cells embedded in 3D collagen type I matrices were exposed to radiation 24 h after seeding into the collagen matrix. For cell survival experiments, cells were irradiated with doses of 1.9, 3.8, 5.7, and 7.6 Gy. For DNA and ALP assays, a dose of 1.9 Gy was applied. Control samples were placed inside the µCT, shielded with a lead cylinder against potential irradiation. Temperature effects on cell survival and ALP expression during a µCT run can thus be excluded. Survival experiments as well as ALP/DNA experiments were all compared with this µCT control.

Cell survival after µCT irradiation

Cell survival after µCT irradiation was determined with a live/dead cytotoxicity kit (Molecular Probes, Eugene, OR, USA). This assay was performed 2 h and 24 h post-irradiation (per dose, and per time point: $n_{samples} = 3$, $n_{control} = 9$). The samples were washed in phosphate buffered saline (PBS, Sigma Aldrich, Basel, Switzerland) and stained for 45 min with 200 µl live/dead staining solution (4 µM ethidium homodimer-1, 2 µM calceinAM in PBS). The samples were then washed in PBS and fixed in 4% glutaraldehyde. Epifluorescence images were taken at five randomly selected locations (area of $\sim 2 \times 1$ mm^2) within the matrix by using a fluorescence microscope (Zeiss Axiovert 135, Feldbach, Switzerland) and the fluorescence for calceinAM was determined with an excitation wavelength of 495 nm and an emission wavelength of 515 nm. For ethidium homodimer-1, an excitation wavelength of 495 nm and an emission wave-

length of 635 nm were used, respectively. The number of surviving cells per total number of cells (live cells plus dead cells, between 30 and 100 cells in total, per location) was determined by manual counting. The cell numbers of the irradiated samples were normalized to the non-irradiated control samples, which were placed into the μCT with lead shielding.

ALP activity assay

Each sample was homogenized in 300 μl lysis solution (0.2% v/v Triton X-100 in 0.56 M 2-amino-methyl-1-propanol, pH 10.0). Total number of samples/controls per time point: $n_{samples} = 10$, $n_{control} = 10$. From each sample an aliquot was used to determine ALP activity. Briefly, 150 μl of the lysed cell suspension was mixed with 20 μl of p-nitrophenyl phosphate solution (74 mg/ml in 0.56 M 2-amino-methyl-1-propanol, pH 10.0) and incubated at 37°C for 30 min. The reaction was stopped by addition of 85 μl 2 N NaOH. The ALP activity was then determined by measuring the absorbance at 405 nm with a spectrometer (Spectronic Genesys 2PC, Thermo Fisher Scientific, Milford, MA, USA).

DNA determination assay

To determine the DNA content per gel, 30 μl of the lysed cell suspension was neutralized by addition of 270 μl TE buffer (100 mM Tris-HCl, pH 7.6, 1 mM EDTA) and centrifuged for 15 min at $11,000 \times g$. Then, 270 μl of sample or DNA standard was mixed with 270 μl Pico Green (Molecular Probes, Eugene, OR, USA) which was diluted 1:200 in TE buffer. Total number of samples/controls per time point: $n_{samples} = 10$, $n_{control} = 10$. Fluorescence was measured in triplicate using a spectrometer (Synergy HT, BioTek Instruments, Inc., Winooski, VT, USA) at 520 nm (excitation wavelength: 480 nm).

Statistical analysis

The cell survival experiments were performed at different doses and are shown as mean values ± standard deviation (total number of samples: per dose and per time point: $n_{samples} = 3$, $n_{control} = 9$). Each sample point was normalized by its corresponding control sample. Comparative analysis was performed with a two-way analysis of variance. To test for significant differences between the dose groups, a pairwise t-test was applied with Holm correction for multiple testing, for both the 2 h and 24 h time groups. To examine significant differences between the 2 h and 24 h time groups within a dose group, we used the Student t-test. Significant differences were accepted for $p < 0.05$.

The results of the DNA and ALP tests were statistically analyzed using a pairwise Wilcoxon rank sum test with Holm correction for multiple testing. Total number of samples/controls per time point: $n_{samples} = 10$, $n_{control} = 10$. Differences between two data sets were considered statistically significant if $p < 0.05$. For all statistical analyses we used "R", a language and environment for statistical computing (R Foundation for Statistical Computing, Vienna, Austria).

Results

Dose measurement and image quality

To investigate the relation between applied dose and image quality, a bovine trabecular bone sample was scanned with μCT applying the doses 0.150 Gy and 0.528 Gy in the standard resolution mode, and 0.458 Gy and 1.980 Gy in the high resolution mode (Figure 1A–C). Better image quality (higher resolution) resulted from higher applied doses (Figure 1A). The gray level images show a better quality by increasing the resolution from 30 to 8 μm, and with changing the imaging mode from standard to high resolution. In addition, the binary images in high resolution mode were found to better display the "real" trabecular structure as compared to the binary images in the standard resolution mode. However, the differences are relatively small and depending on the application a low resolution mode can yield reasonable results at an acceptable dose. We show that the relation between dose and image quality, here represented as nominal resolution, can be modeled as a power law with exponents 1.74, 1.76, and 2.03 for the standard, medium, and high resolution mode, respectively (Figure 1B,C).

### Cell survival after μCT imaging is dose- and time-dependent

To examine the effects of high-resolution μCT imaging on a cellular level, we first evaluated the survival rate 2 h and 24 h post-irradiation, with doses of 1.9, 3.8, 5.7, and 7.6 Gy, respectively, using custom-made PMMA sample holders. We found no significant increase in cell death for a dose of 1.9 Gy immediately (2 h) after irradiation as compared to the non-irradiated control group. However, 24 h post-irradiation, cell survival was significantly decreased by 15% over the control group. Doses after exposure to 3.8 Gy and 5.7 Gy resulted in survival rates of around 80%. Although we did not find a significant decrease in cell survival after exposure to 3.8 Gy between 2 h and 24 h post-irradiation, we demonstrate a significant decrease after exposure to 5.7 Gy by 15%. The highest dose of 7.6 Gy decreased the survival rate of the cells by around 40% 24 h post-irradiation as compared to non-irradiated control samples. Nevertheless, no significant difference between 2 h and 24 h post-irradiation was observed for this highest dose.

Time-dependent decrease of ALP activity per cell

To further investigate the cellular effects of high-resolution μCT imaging, we applied a dose of 1.9 Gy and analyzed ALP activity. When ALP activity was normalized with the DNA content of the same sample, we found no significant increase in ALP activity 2 days post-irradiation, but a significant decrease to approximately 60% at 7 days (Figure 2).

Discussion

This is one of the first studies investigating the effect of ionizing radiation of high-resolution μCT measurements on
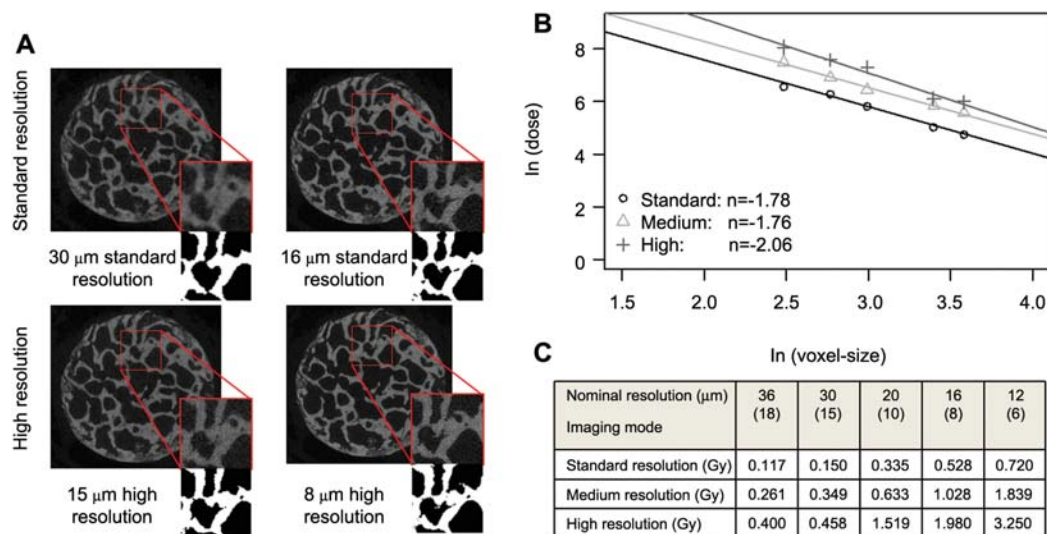
**Figure 1**   Relation of μCT image quality and applied dose.

(A) μCT images of a bovine trabecular bone sample. Insets show higher magnifications and the corresponding binary images, respectively. These scans were performed in four different modes: standard resolution at 30 μm and 16 μm nominal resolution (voxel size), and high resolution at 15 μm and 8 μm nominal resolution. The nominal resolution corresponds to the scanner settings and not to the actual spatial resolution. (B) The relation between dose and image quality (here given as nominal resolution) can be modeled as a power law with exponents 1.74, 1.76, and 2.03, for standard, medium and high resolution mode, respectively. (C) Radiation dose in function of the imaging mode. For all cell experiments the medium resolution mode at 20 μm nominal resolution was used, but with a threefold integration time resulting in a calculated base dose of 1.9 Gy per measurement. To achieve the higher doses of 3.8, 5.7, and 7.6 Gy, the base measurement was repeated 2, 3, and 4 times, respectively.

a cellular level by using a 3D tissue-like model system. Using our model system, the results indicate that μCT imaging with doses as low as 1.9 Gy, which is required to obtain a reasonable image quality, can induce irreparable damages on the cellular level.

The dose applied by a μCT measurement depends on the imaging mode and scanner settings, which are adapted to the features of interest. For instance, if bone volume density is of interest, a relatively low image quality could provide sufficiently good results. However, to capture alterations on the bone surface, a relatively good image quality with high resolution is required, which could be needed to expose the tissue to doses of 2 Gy or even higher. In such cases, the applied dose is not negligible and could result in potential side effects on the cellular level as demonstrated in Figures 2 and 3.

Our results indicate that the effects of ionizing radiation on survival of the pre-osteoblastic MC3T3-E1 cells are different in our 3D model system with collagen type I matrices mimicking natural bone-like tissue as compared to 2D culture plates. We show considerably higher survival rates when similar doses are applied as previously reported for 2D studies (Figure 3A,B). For instance, it was demonstrated that osteoblast-like cells from the calvarium of newborn rats survived only by 60%, 35%, and less than 5% on a 2D surface when 2, 4, and 6 Gy, respectively, were applied to the culture [5]. The reason for this difference is unclear. We speculate that the 3D organization of the cells mimicking a more natural tissue-like environment than a 2D culture could have a

protective effect, but also supports repair mechanisms more efficiently after irradiation damage. In addition, shielding effects of the PMMA sample holder might not be totally excluded.
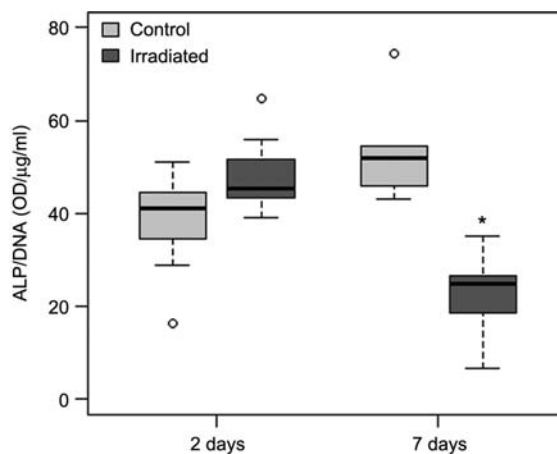
Figure 2   Time-dependent decrease of ALP activity after exposure to 1.9 Gy radiation dose.

Although no significant alteration in the 2 day post-irradiation group was found, the ALP activity was significantly decreased by 60% at 7 days post-irradiation. In these box plots, the box represents/contains 50% of the data, and the whiskers show the data range excluding extreme values that are shown as single data points. Differences between two data sets were considered statistically significant if $p < 0.05$ and are indicated in the Figure by a star.
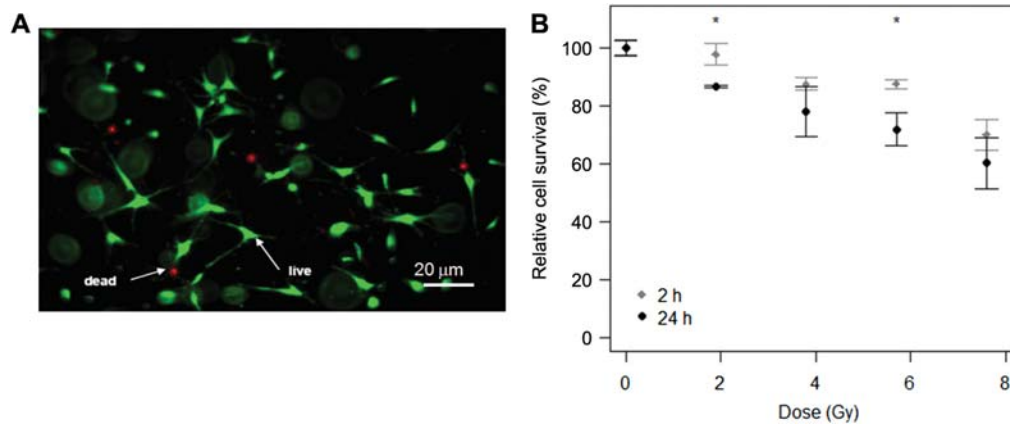
Figure 3 Survival of pre-osteoblastic MC3T3-E1 cells in 3D collagen matrices after μCT imaging.
(A) Representative image of pre-osteoblastic cells in 3D collagen matrices 24 h post-irradiation. (B) Dose- and time-dependent survival 2 h and 24 h after irradiation as assessed by quantifying live/dead cell staining. At a dose of 2 Gy, which is commonly applied for *in vitro* and *in vivo* imaging, the fraction of surviving cells 24 h after irradiation is significantly lower than at 2 h. The highest dose applied (8 Gy) still resulted in survival of >60% both at 2 h and 24 h after irradiation. The survival rates at each dose were normalized by the survival rates of the control samples and are shown as mean values ± standard deviation ($n_{samples}=3$, $n_{controls}=9$; images were taken at five randomly selected/representative locations within the matrix). Significant differences were accepted if $p<0.05$. * Indicates significantly different data between 2 h and 24 h.

Expression of ALP activity is a relevant marker in the early differentiation process of MC3T3-E1 pre-osteoblastic cells towards mature osteoblasts as it is upregulated with proceeding maturation [18]. We show here a time-dependent decrease of ALP activity after exposure to radiation (Figure 2). Although no significant alteration was found 2 days post-irradiation, the ALP activity was significantly decreased at 7 days by around 60%. We speculate that differentiation and maturation processes could be inhibited after irradiation. However, it is not clear by which mechanisms the ALP activity is influenced by irradiation. It could be as a result of altered cytokine expression profiles, by the irradiation directly or by combined processes [6]. Other authors found inhibition of differentiation, when exposing mature osteoblasts in a 2D environment to 4 Gy doses. In a study by Hagenmüller et al., ALP activity normalized to the DNA content was shown to be decreased by around 20% after 3 days of irradiation, around 60% after 6 days, and around 70% after 9 days. However, a study using 3D scaffolds prepared from silk fibroin and human mesenchymal stem cells did not demonstrate alterations in ALP activity after repeated high-resolution μCT imaging over a period of 28 days [13]. The reasons for these controversial results on the ALP activity could include different study designs including different cell types, radiation doses, the different times between the μCT imaging and the ALP activity assays, which can allow DNA repair processes in some cases, as well as the different biophysical and biochemical properties of the 3D scaffolds used in the respective studies.

The direct transfer of the results obtained in this study into *in vivo* experiments might not be possible; however, the *in vitro* model system applied here allows conclusions for *in vitro* tissue engineered constructs or bone chambers (i.e., critical dose). The critical dose for *in vivo* applications needs to be assessed with the respective *in vivo* models, specifically the effects on bone tissue growth, healing, and turnover. Potential immune reactions, vascularization of the tissue, and potential shielding effects of the surrounding tissue can affect the critical dose *in vivo*.

Conclusion

We have established a model system allowing the monitoring of 3D tissue engineered constructs using μCT imaging. Our results indicate significant impairments on the cellular level after imaging with high-resolution μCT in a time- and dose-dependent manner. Results from this study indicate that imaging with high-resolution μCT with doses as low as 1.9 Gy, which is required to obtain a reasonable image quality, can yield irreparable damages on the cellular level.

It is therefore recommended to use the lowest resolution necessary in monitoring studies of bone chambers and 3D tissue engineered bone-like constructs. Future studies could include other cells such as mesenchymal cells present in bone tissue and/or different scaffolds, as well as longitudinal monitoring. Longitudinal animal studies could be performed to assess a critical *in vivo* dose to avoid potential damages on the cellular level.

Acknowledgements

Author disclosure statement

The authors declare no competing financial interests.

References

[1] Abbott A. Cell culture: biology's new dimension. Nature 2003; 424: 870–872.

[2] Arnold M, Kummermehr J, Trott KR. Radiation-induced impairment of osseous healing: quantitative studies using a standard drilling defect in rat femur. Radiat Res 1995; 143: 77–84.

[3] Bonse U, Busch F, Günnewig O, et al. 3D computed X-ray tomography of human cancellous bone at 8 microns spatial and 10(-4) energy resolution. Bone Miner 1994; 25: 25–38.

[4] Cartmell S, Huynh K, Lin A, Nagaraja S, Guldberg R. Quantitative microcomputed tomography analysis of mineralization within three-dimensional scaffolds in vitro. J Biomed Mater Res A 2004; 69: 97–104.

[5] Dare A, Hachisu R, Yamaguchi A, Yokose S, Yoshiki S, Okano T. Effects of ionizing radiation on proliferation and differentiation of osteoblast-like cells. J Dent Res 1997; 76: 658–664.

[6] Dudziak ME, Saadeh PB, Mehrara BJ, et al. The effects of ionizing radiation on osteoblast-like cells in vitro. Plast Reconstr Surg 2000; 106: 1049–1061.

[7] Elsdale T, Bard J. Collagen substrata for studies on cell behavior. J Cell Biol 1972; 54: 626–637.

[8] Friedrich J, Seidel C, Ebner R, Kunz-Schughart LA. Spheroid-based drug screen: considerations and practical approach. Nat Protoc 2009; 4: 309–324.

[9] Gal TJ, Munoz-Antonia T, Muro-Cacho CA, Klotch DW. Radiation effects on osteoblasts in vitro: a potential role in osteoradionecrosis. Arch Otolaryngol Head Neck Surg 2000; 126: 1124–1128.

[10] Genant HK, Engelke K, Fuerst T, et al. Noninvasive assessment of bone mineral and structure: state of the art. J Bone Miner Res 1996; 11: 707–730.

[11] Goldwein JW. Effects of radiation therapy on skeletal growth in childhood. Clin Orthop Relat Res 1991; 262: 101–107.

[12] Griffith LG, Swartz MA. Capturing complex 3D tissue physiology in vitro. Nat Rev Mol Cell Biol 2006; 7: 211–224.

[13] Hagenmüller H, Hofmann S, Kohler T, et al. Non-invasive time-lapsed monitoring and quantification of engineered bone-like tissue. Ann Biomed Eng 2007; 35: 1657–1667.

[14] Hofmann S, Hagenmüller H, Koch AM, et al. Control of in vitro tissue-engineered bone-like structures using human mesenchymal stem cells and porous silk scaffolds. Biomaterials 2007; 28: 1152–1162.

[15] Kirshner J, Thulien KJ, Martin LD, et al. A unique three-dimensional model for evaluating the impact of therapy on multiple myeloma. Blood 2008; 112: 2935–2945.

[16] Lanza RP, Langer R, Vacanti JP. Principles of tissue engineering. San Diego, CA: Academic Press 2007.

[17] Majumdar S, Genant HK, Grampp S, et al. Correlation of trabecular bone structure with age, bone mineral density, and osteoporotic status: in vivo studies in the distal radius using high resolution magnetic resonance imaging. J Bone Miner Res 1997; 1: 111–118.

[18] Rodan GA, Rodan SB. Expression of the osteoblastic phenotype. In: Peck WA, editor. Advances in bone and mineral research. Annual II. Amsterdam: Excerpta Medica 1984: 244–285.

[19] Rüegsegger P, Koller B, Müller R. A microtomographic system for the nondestructive evaluation of bone architecture. Calcif Tissue Int 1996; 58: 24–29.

[20] Thurner P, Müller R, Raeber G, Sennhauser U, Hubbell JA. 3D morphology of cell cultures: a quantitative approach using micrometer synchrotron light tomography. Microsc Res Tech 2005; 66: 289–298.

[21] U.S. Department of Health and Human. U.S. Government web site for organ and tissue donation and transplantation: www.organdonor.gov.

[22] Weber FE, Eyrich G, Grätz KW, Thomas RM, Maly FE, Sailer HF. Disulfide bridge conformers of mature BMP are inhibitors for heterotopic ossification. Biochem Biophys Res Commun 2001; 286: 554–558.

[23] Zehbe R, Goebbels J, Ibold Y, Gross U, Schubert H. Three-dimensional visualization of in vitro cultivated chondrocytes inside porous gelatine scaffolds: a tomographic approach. Acta Biomater 2010; 6: 2097–2107.